

State Space Model Optimization for Hyperbilirubinemia Management using Truncated Balance Realization

Tai BANDISAK*, Sawit TANTHANUCHT and Booncharoen WONGKITTISUKSA

Department of Electrical Engineering, Faculty of Engineering, Prince of Songkla University, Songkhla 90110, Thailand

(* Corresponding author's e-mail: bandisak@hotmail.com, bandisak.t@gmail.com)

Received: 26 September 2014, Revised: 2 April 2015, Accepted: 24 May 2015

Abstract

Neonatal jaundice is a high bilirubin accumulation experienced in 60 % of newborns leading to permanent brain damage. However, bilirubin reduction time for an appropriate treatment is difficult to determine because of complicated bilirubin kinetics. This article presents a compartmental model optimization of bilirubin. The truncated balanced realization is employed to reduce complexity of the conventional bilirubin model. The compartments are determined by absolute value and argument analysis that are also able to simplify the conventional 3-compartment model to a 2-compartment model. The proposed models are verified with Berk and Brown 3-compartment models with focuses on the half-life and the trough point. Verification results showed that the half-life point of the optimized model is 20 min faster and the processing time to the trough point is approximate 8 % slower than the Berk model. In comparison with the Brown model, the half-life of the optimized model is similar the Berk model, and the processing time to the trough is 5 % slower than the original model. The proposed algorithm simplifies the complex compartmental models yielding comparable results, though it has to be traded off with a little slower time for the trough, and could well be developed into a high performance neonatal jaundice treatment system.

Keywords: Bilirubin, compartmental model, neonatal jaundice, model order reduction, truncated balance realization

Introduction

Bilirubin is a yellowish substance, soluble conjugated bilirubin (CB) and insoluble unconjugated bilirubin (UCB), produced from red blood cell catabolism. Neonatal jaundice is a case of high accumulation of bilirubin leading to kernicterus that permanently damages the brain, it occurs in 60 % of newborns [1]. This disease leads to 10 % mortality and 70 % long-term morbidity [2]. The gold standard method to determine bilirubin concentrations is the Total Serum Bilirubin (TSB) analysis which is used to classify the risk to neonates. The process need blood drilling with the side effects from multiple blood sampling. If the treatment period cannot be accurately predicted by some bilirubin samples, then TSB are evaluated for management. Though non-invasive bilirubin measurements to reduce the needs for blood samplings are conducted and compared [3,4] these methods cannot be used during phototherapy because the internal characteristics of neonates are changed by light intensity [5]. The conventional medical treatment of this condition is phototherapy, using light to convert UCB to water soluble CB that can then be excreted via the kidneys and gut [6].

The pathways of serum bilirubin motivated for the bilirubin management problems. Berk [7] investigated bilirubin kinetics in young adults. They presented a 3-compartment model: a plasma pool, an extravascular pool and a hepatic pool. This model was used to explain the rate of change in bilirubin-¹⁴C, focusing on the unconjugated bilirubin (**Figure 1**).

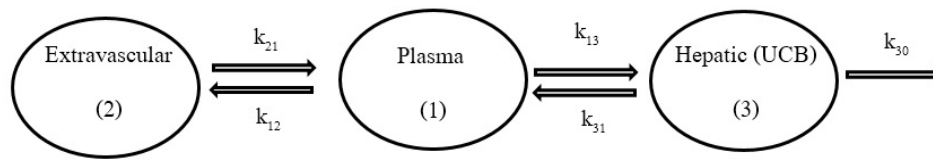


Figure 1 Berk's bilirubin three-compartment model [7].

Brown [8] presented another model with 5 compartments consisting of plasma, extravascular, hepatic, intestine and gut compartments (**Figure 2**). This model was based on kinetics tracers related to the Berk model. Brown simplified their original model (**Figure 2**) down to a 3-compartment model (compartment 1, 2, and 3) and 2 2-compartment models (compartment 1+2 and compartment 3; compartment 1+3 and compartment 2). Moreover, the model complexity had also been reduced by parameter estimation [9-11].

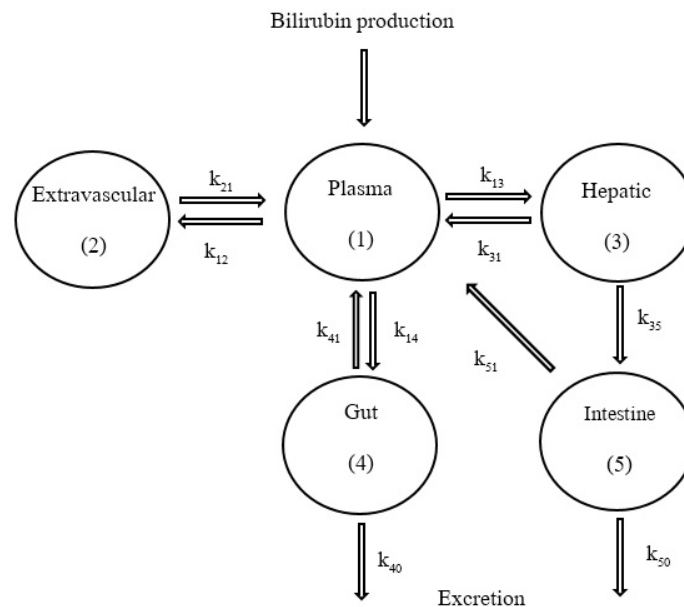


Figure 2 Brown's bilirubin compartment model [8].

The compartment model can be explained with first order differential equations and the fourth order Runge-Kutta algorithm was applied to solve numerically [12,13]. Eqs. (1) - (3) explain the bilirubin kinetics of the model shown in **Figure 1**.

$$\frac{dC_1(t)}{dt} = -(k_{12} + k_{13})C_1(t) + k_{21}C_2(t) + k_{31}C_3(t) + P, \quad (1)$$

$$\frac{dC_2(t)}{dt} = (k_{12})C_1(t) - (k_{21})C_2(t), \quad (2)$$

$$\frac{dC_3(t)}{dt} = k_{13}C_1(t) + (k_{31} + k_{30})C_3(t), \quad (3)$$

where parameters C_1, C_2, C_3 are the concentration of compartment 1, 2 and 3, respectively; variable k_{ij} is a rate constant from compartment i to compartment j ; P is the bilirubin production rate and, k_{30} is bilirubin excretion rate.

The compartment models were too complicated; hence model optimizations were used for simplification. The method of model optimization based on the underlying physiology include: parameter estimation and curve fitting; pole cancellation; and truncated balanced realization.

The parameter estimation and curve fitting [14,15] was used to simplify models with estimation that depend on the relationship of system inputs and outputs and it cannot be used in high complexity models. This method lacks flexibility for the system input variation, hence were not suited for optimization of complicated physiology models. The pole cancellation was used to optimize control systems [16]. This simplified model was structurally different from the original model, loses its physiological interpretation and thus was not suited for this application. The truncated balanced realization (TBR) based on Hankel singular values [17-20] for the current modeling problems can be used to optimize highly complicated models involving large numbers of variables such as those presented in the original model. Truncated balanced realization (TBR) with Hankel singular values [17-20], detailed in the methodology section, had been used very successfully in electrical control systems. In this research, we derived an optimal reduced order compartmental model of bilirubin based on TBR methods in order to simplify the model for bilirubin prediction.

Methodology

This article, model optimization and validation, was based on the iatrogenic case data of the original bilirubin compartmental models of Berk and Brown (**Figures 1 and 2**). TBR presented in [19,20] was used for model simplification. The bilirubin compartmental model was initially transformed to a state space representation shown in Eqs. (4) and (5).

$$\dot{x}(t) = \mathbf{A}x(t) + \mathbf{B}u(t); x(0) = x_0, \quad (4)$$

$$y(t) = \mathbf{C}x(t) + \mathbf{D}, \quad (5)$$

where (t) is the processing time; \mathbf{A} is the system matrix, \mathbf{B} the input matrix, \mathbf{C} the output matrix, and \mathbf{D} the direct transmission matrix; $x(t)$ is the internal state of the compartment model represented by k_{ij} ; $u(t)$ and $y(t)$ are respectively the controlled input and the observable output of the system determined by the 1st compartment. Parameters of Eqs. (1) - (3) were transformed to a state space model described by Eq. (6).

$$\mathbf{A} = \begin{bmatrix} -(k_{12} + k_{13}) & k_{21} & k_{31} \\ k_{12} & -k_{21} & 0 \\ k_{13} & 0 & -(k_{31} + k_{30}) \end{bmatrix}, \quad (6)$$

$$\mathbf{B} = [1 \ 0 \ 0]^T, \mathbf{C} = [1 \ 0 \ 0], \mathbf{D} = [0],$$

For model optimization procedure, we used the procedure of TBR [19,20]. First, the controllability (\mathbf{W}_c) and observability (\mathbf{W}_o) Gramian matrices were determined from linear Eqs. (7) and (8);

$$\mathbf{A}\mathbf{W}_c + \mathbf{W}_c\mathbf{A}^T = -\mathbf{B}\mathbf{B}^T, \quad (7)$$

$$\mathbf{A}^T\mathbf{W}_o + \mathbf{W}_o\mathbf{A} = -\mathbf{C}^T\mathbf{C}, \quad (8)$$

where \mathbf{A} is stable matrix [21]. Then, their Cholesky factors [19,20] were calculated to comply with Eqs. (9) and (10);

$$W_c = L_c L_c^T, \tag{9}$$

$$W_o = L_o L_o^T, \tag{10}$$

where L_c and L_o are the lower triangular Cholesky factors of W_c and W_o , respectively.

Next, the Hankel singular values in Eq. (11) were computed using Cholesky factors. The balancing transformation (T) was defined by Eq. (12) and its inverse complied with Eq. (13).

$$UAV = L_o^T L_c, \tag{11}$$

$$T = L_c V A^{-1/2}, \tag{12}$$

$$T^{-1} = A^{-1/2} U^T L_o^T, \tag{13}$$

where T must not be a singular matrix [22]; A is a diagonal matrix with positive singular values on the diagonal, while U and V are orthogonal matrices corresponding to rotations of the coordinate axes.

This balancing transformation (T) was implemented to balance the state space [19,20] by $\hat{A} = T^{-1}AT$, $\hat{B} = T^{-1}B$, $\hat{C} = CT$. Then the Hankel singular values were computed for model reduction by removing the smaller insignificant ones. The Hankel singular values represent the state importance of the model that was used to indicate eradication of those states that were least significant. Finally, the modified model was verified with the original models using absolute value and argument analyses to identify the appropriate number of the optimized compartment models.

Results

Hankel singular values are calculated (**Table 1**) to initially assess the importance of the compartment and to remove the less important ones.

Table 1 Hankel singular values from the Berk model.

Compartment	Hankel singular values
1	26.4746
2	6.6826
3	1.4279

The Hankel singular values indicate the important states (11). From **Table 1**, the value of the 3rd compartment is least significant and this compartment is removed. The optimum compartment number is determined by absolute and argument analyses.

In the comparison between Berk’s original compartment model and the proposed model (**Figure 3**), absolute value and argument are used to determine the optimum compartment number, focusing on the observable changes in the argument curve. Thus, a 2-compartment model is the optimum model in this case because there are 2 flexural changes exhibited on the argument curve.

In the sense of the criteria from which the TBR is derived by [19,20], both reduced order models are optimal simplifications of the 3-compartment model. The bilirubin concentration results in the 1st compartment of the modified models are similar to that from the original model. Model verification is subsequently conducted on both models. Berk’s optimized model, and the 2-compartment is explained by state space model in Eq. (14).

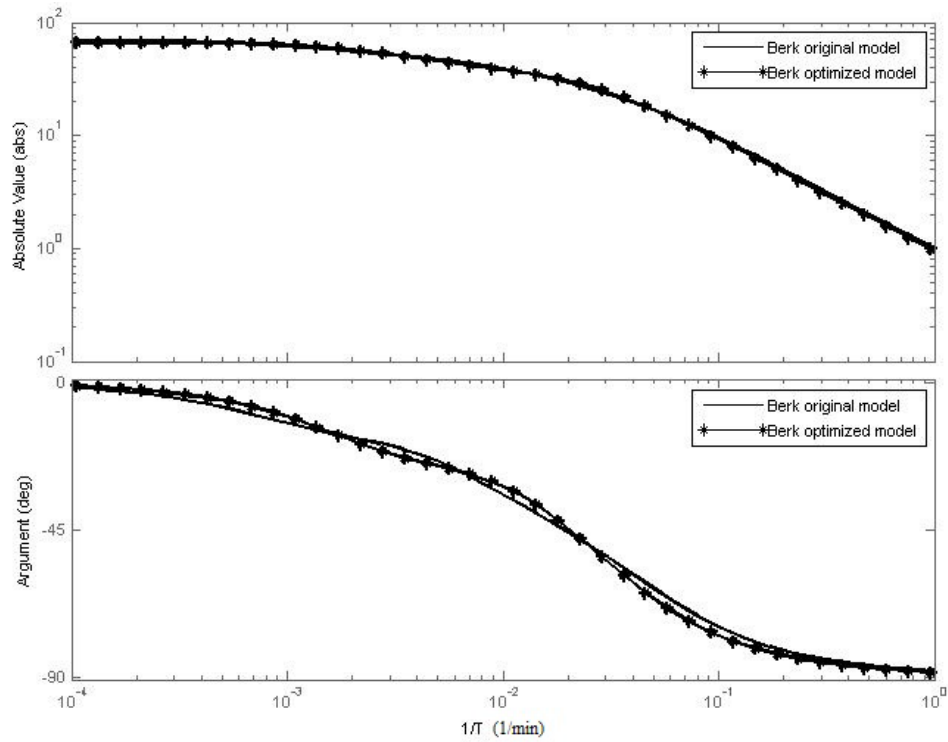


Figure 3 Comparison by absolute value and argument of Berk's original compartment model results and that of the proposed simplified model.

$$\hat{\mathbf{A}} = \begin{bmatrix} -0.02167 & 0.003859 \\ 0.0123 & -0.005107 \end{bmatrix}, \quad (14)$$

$$\hat{\mathbf{B}} = [0.9425 \quad -0.1613]^T, \quad \hat{\mathbf{C}} = [1 \quad 5.811 \times 10^{-6}], \quad \hat{\mathbf{D}} = [0].$$

The result in **Figure 4** shows that bilirubin concentrations of the optimized model and the Berk's original model have similar trends and behaviors, inferring that the optimized model (2-compartment model) accurately represent the original models.

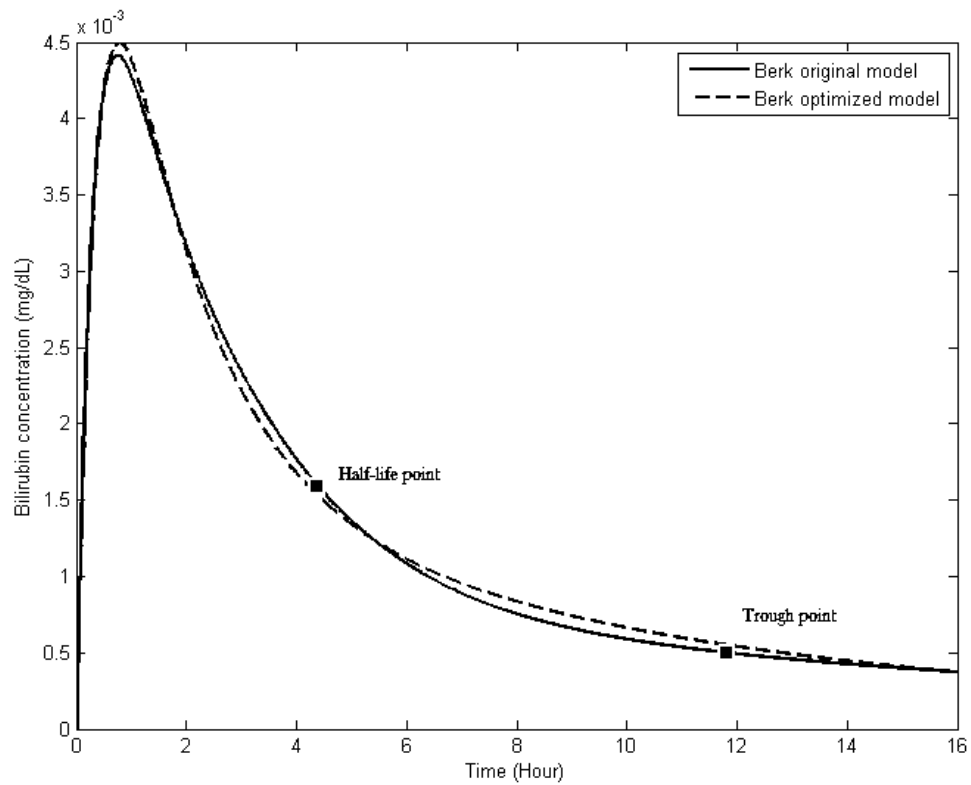


Figure 4 Verification of results between the optimized model and Berk’s compartment model.

In the Brown’s compartment model, the Hankel singular values are calculated and analyzed to evaluate the importance of the internal model relationship. The result of the Hankel singular values from the Brown model (**Table 2**) are similar to the Berk model.

Table 2 Hankel singular values from the Brown model.

Compartment	Hankel singular values
1	17.4231
2	3.0334
3	1.1435

In this case, the value of the 3rd compartment is least significant and this compartment can be removed correlating to the number of curve changes of the argument shown in **Figure 5**.

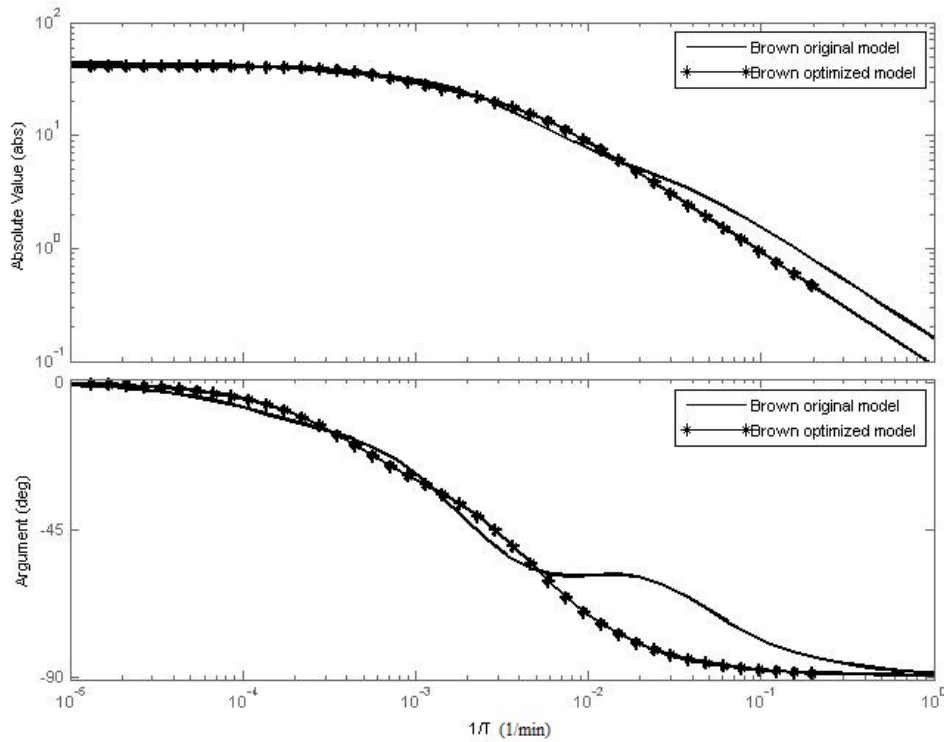


Figure 5 Comparison by absolute value and argument of Brown's original compartment model results and that of the proposed simplified model.

The optimized model is explained using Eq. (15) and verified with the Brown's original model (**Figure 6**), subsequently.

$$\begin{aligned} \hat{\mathbf{A}} &= \begin{bmatrix} -0.02029 & 0.00315 \\ 0.02287 & -0.008653 \end{bmatrix}, \\ \hat{\mathbf{B}} &= [0.5788 \quad -0.2456]^T, \quad \hat{\mathbf{C}} = [1 \quad 3.105 \times 10^{-5}], \quad \hat{\mathbf{D}} = [0]. \end{aligned} \quad (15)$$

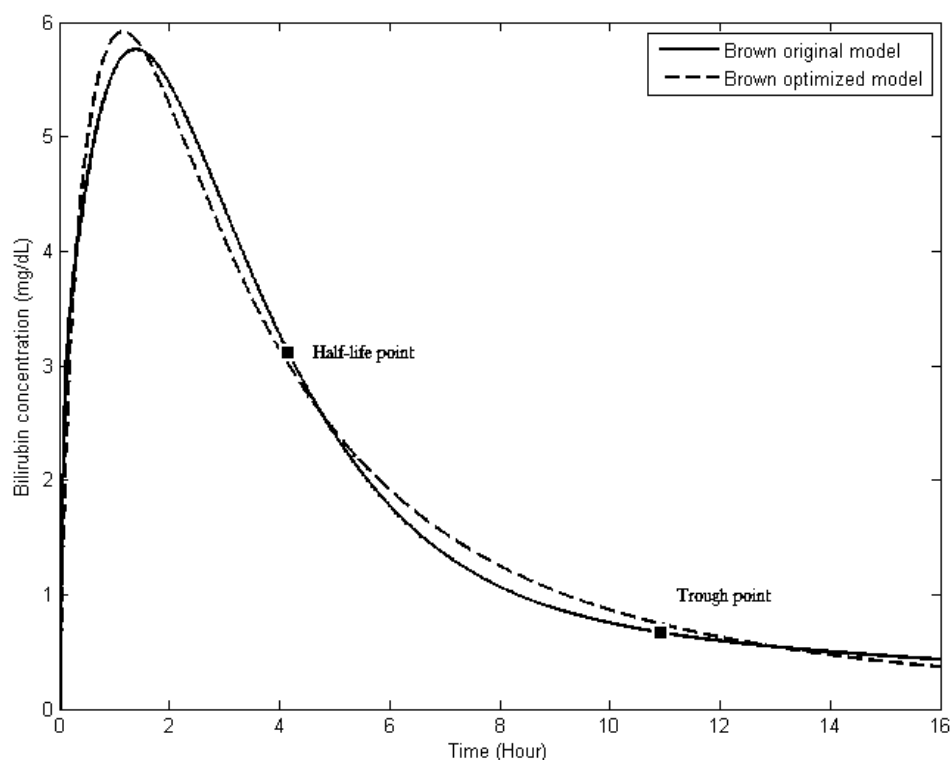


Figure 6 Verification of results between the optimized model and Brown's compartment model.

Discussions

Complex number analysis is applied to verify the optimized model in the absolute values and the arguments. This method determines the number of optimum compartments in the model optimization procedure. In our experiment, 2 points of inflection on the curve are found on the argument inferring a 2-compartment model. The verification results show that the half-life values of the optimized model and the original model are of similar magnitude. The proposed models agree with the distribution rate and the decreasing rate based on the half-life point ($t_{1/2} = \frac{\ln 2}{k}$), where k is the slope and also on the trough point. The trough point is a threshold point, taken as the time when bilirubin concentration decreases down to 10 % of the maximum value. In this investigation, the trough point is the main point to predict the time bilirubin decreases in neonatal jaundice. The accuracy of the results are dependent on the similarity of the absolute value and argument between the original model and the optimized model.

The trough point time obtained from the Berk model is close to 12 h whereas the proposed model is about an hour slower. The half-life point from the model is approximate 4.5 h while the optimized model is 20 min faster. For the Brown model, a hypothetical maximum concentration of approximate 6 mg/dL the trough point is close to 11 h and that from the proposed model is about 0.5 h slower; the half-life point from the model is a little over 4 h while the optimized model is approximate 15 min faster.

Comparing with both the Berk and the Brown model, the proposed algorithm produces similar results within a tolerable duration. The trough points reached from the proposed models are approximately 5 - 8 percent more than those obtained from the Berk and the Brown models. The half-life check point time from the proposed models have been proven to be a little faster.

Conclusions

We perform an optimal model reduction by TBR to simplify a compartmental bilirubin model. This approach reduces the 3-compartment original models to a 2-compartment model. For model verification, we compare the simplified model with the original model and the other compartmental bilirubin models. It indicates that the original model was closely imitated by the simplified model. The trough point and the half-life point obtained from the optimized model and the original model are tolerably comparable. The TBR method is thus suitable for simplification of multi-compartmental models. In future work, this approach could be used to optimize the complex models, such as glucose-insulin kinetic models and anesthesia control system, to strive for better medical managements.

Acknowledgements

The authors would like to thank Assoc. Prof. Seppo Karrila from the Prince of Songkla University (PSU) Surat Thani Campus, Dr. Warit Wichakool from the PSU Department of Electrical Engineering, and the PSU Research and Development Office (RDO) for insightful discussions and assistance. Research scholarship from the PSU Graduate School is gratefully appreciated. Provision on polishing up the article by a retired PSU engineering lecturer Mr. Wiwat Sutiwipakorn is also greatly acknowledged.

References

- [1] VK Bhutani, GR Gourley, S Adler, B Kreamer, C Dalin and LH Johnson. Noninvasive measurement of total serum bilirubin in a multiracial predischarge newborn population to assess the risk of severe hyperbilirubinemia. *Pediatrics* 2000; **106**, 17-25.
- [2] S Ip, M Chung, J Kulig, R O'Brien, R Sege, S Glicken, MJ Maisels, J Lau and the Subcommittee on Hyperbilirubinemia. An evidence-based review of important issues concerning neonatal hyperbilirubinemia. *Pediatrics* 2004; **114**, 130-53.
- [3] W Janjindamai, A Pochanukul and P Chanvitan. Transcutaneous bilirubin measurements in full-term neonate. *Songkla Med. J.* 2001; **19**, 61-7.
- [4] S Sanpavat and I Nuchprayoon. Noninvasive transcutaneous Bilirubin as a screening test to identify the need for serum Bilirubin assessment. *J. Med. Assoc. Thai* 2004; **87**, 1193-8.
- [5] E Zecca, G Barone, DD Luca, R Marra, E Tiberi and C Romagnoli. Skin bilirubin measurement during phototherapy in preterm and term newborn infants. *Early Hum. Dev.* 2009; **85**, 537-40.
- [6] MJ Maisels and AF McDonagh. Phototherapy for Neonatal Jaundice. *New Engl. J. Med.* 2008; **358**, 920-8.
- [7] PD Berk, RB Howe, JR Bloomer and NI Berlin. Studies of bilirubin kinetics in normal adults. *J. Clin. Investig.* 1969; **48**, 2176-90.
- [8] RF Brown and KR Godfrey. Problems of determinacy in compartmental modeling with application to bilirubin kinetic. *Math. Biosci.* 1978; **40**, 205-24.
- [9] L Campello and C Cobelli. Parameter estimation of biological stochastic compartmental models-an application. *IEEE Trans. Biomed. Eng.* 1978; **25**, 139-46.
- [10] S Audoly, LD Angio, MP Saccomani and C Cobelli. Global identifiability of linear compartmental models - A computer algebra algorithm. *IEEE Trans. Biomed. Eng.* 1998; **45**, 36-47.
- [11] B Moore. Principal component analysis in linear systems: Controllability, observability, and model reduction. *IEEE Trans. Automat. Contr.* 1981; **26**, 17-32.
- [12] CJ Mullon, CM Tosone and R Langer. Simulation of bilirubin detoxification in the newborn using an extracorporeal bilirubin oxidase reactor. *Pediatr. Res.* 1989; **26**, 452-7.
- [13] SM Dunn, A Constantinides and PV Moghe. *Numerical Methods in Biomedical Engineering*. 1st ed. Academic Press, 2005, p. 209-32.
- [14] HWA Berkelmans, BWM Moeskops, J Bominaar, PTJ Scheepers and FJM Harren. Pharmacokinetics of ethylene in man by on-line laser photoacoustic detection. *Toxic. Appl Pharmacol.* 2003; **190**, 206-13.

- [15] D Koushik and SC Mishra. Non-invasive estimation of size and location of a tumor in a human breast using a curve fitting technique. *Int. Comm. Heat Mass Tran.* 2014; **56**, 63-70.
- [16] K Ogata. *Modern Control Engineering*. 5th Ed. Pearson, New Jersey, 2008, p. 658-97.
- [17] BY Sheldon, XD Tan, L Zhou, J Chen and R Shen. Decentralized and passive model order reduction of linear networks with massive ports. *IEEE Trans. VLSI Syst.* 2012; **20**, 865-77.
- [18] M Kamon, F Wang and J White. Generating nearly optimally compact models from Krylov-Subspace based reduced-order models. *IEEE Trans. Circ. Syst. II* 2000; **47**, 239-48.
- [19] AJ Laub, MT Heath, CC Paige, and RC Ward. Computation of system balancing transformations and other applications of simultaneous diagonalization algorithms. *IEEE Trans. Automat. Contr.* 1987; **32**, 115-22.
- [20] JR Phillips, L Daniel and LM Silveira. Guaranteed passive balancing transformations for model order reduction. *IEEE Trans. Comput. Aided Des. Integrated Circ. Syst.* 2003; **22**, 1027-41.
- [21] T Kailath. *Linear Systems*. Prentice-Hall, New Jersey, 1980.
- [22] G Strang. *Linear Algebra and Its Applications*. 4th ed. Thomson, USA, 2006, p. 1-58.